Implementation and validation of a new SAR data imaging processor based on efficient time-domain focusing core

Francesco Tataranni, Antonella Gallipoli (INNOVA Consorzio)

VH-RODA: Very High-resolution Radar & Optical Data Assessment workshop and CEOS SAR 2019 workshop

ESA/ESRIN Frascati, ITALY 18–22 November 2019

Company Profile

SME Company Founded in 1989

Mission

Born in the space sector in the **earth observation field**, INNOVA is specialized in remote sensing technologies and specifically in the processing of satellite images acquired by **synthetic aperture radar (SAR)** for civil and defense applications.
In recent years the company has expanded its activity by developing services and applications in the field of Intelligent Transport Systems.

Organization

The company consists of 2 **Business Unit**:

- **Earth Observation**
- Innovambiente® (Waste Management)

Group

The company is participated by:

- Cooperativa EDP La Traccia
- Lucana Sistemi Srl
- HSH Informatica & Cultura Srl

and is part of a larger group of companies specialized in the development of technological systems and applications in various sectors.
The group can rely on a team of about 150 resources with highly specialized skills and a turnover of over 10M€.

Earth Observation Projects

INNOVA since its foundation is engaged in the field of Earth Observation, since 2001 is part of the industrial structure involved in the main national space program COSMO Skymed (CSK) and, in continuity, in the program COSMO Second Generation (CSG).

Main Industrial Projects

- **COSMO-SkyMED Second Generation – CSG – Development of SW components for the generation of RAW data starting from the downlinked L0File and the generation of SAR standard L1 products starting from the RAW data for the Stripmap and the Spotlight acquisition modes (2009, ongoing)**
- **COSMO SkyMED – CSK – Development of SW components for the generation of RAW data starting from the downlinked L0File and the generation of SAR standard products starting from the raw data for the Civilian and Defence User Ground Segments and Commercial/Portable User Terminal (dal 2001, maintenance phase ongoing)**
- **COSMO SkyMED – CSK – Development of standard product DEGradation ENVironment (DGRENV) for the Defence User Ground Segment (dal 2013, maintenance phase ongoing)**
- **Logistic Support in the Development and Maintenance of the COSMO Corner Reflector test sites in the Basilicata Region.**
- **Software ROSA per OCEANSAT-2 (2007-2011)**

Main R&D Projects

- **2° Call ASI for SME – (2012-2015)**
- **GIANT – ESA GSTP (2010-2014) *GMSPAZIO INNOVA Atmospheric New Toolkit***
- **PRIMI «Progetto pilota Inquinamento Marino da Idrocarburi» – ASI R&D Oil Spill Detection (2007-2010)**
- **ASI-Grid (2007-2010)**
- **InterRisk – EU FP6 (2006-2010) - Interoperable GMES Services for Environmental Risk Management in Marine and Coastal Areas of Europe**

Main Skills

- **SAR processing algorithm design for Spotlight and Stripmap acquisition modes**
- **Design, Implementation and Testing of High Quality and High Performance Software for operational environments in both civilian and military space missions using the ECSS/ESA standards.**

Earth Observation Lab

INNOVA carries out research and development activities even with the collaboration of other Italian and European companies and research institutes.
Our activities of R&D for the period 2018-2020 include:

- Development of image formation algorithms for new generation SAR sensors
- Development of tools for SAR image quality analysis
- Design and prototyping of the platform for integrated management of SAR data
- Deep Learning applied to the processing of SAR data

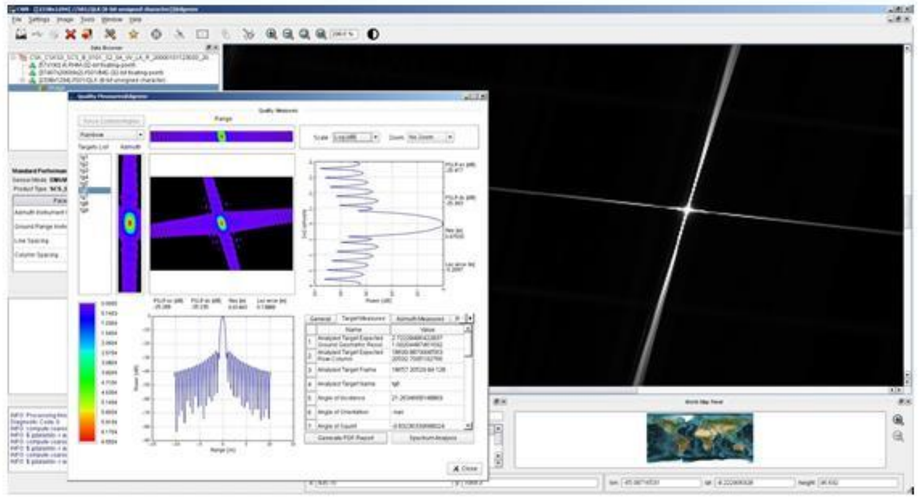

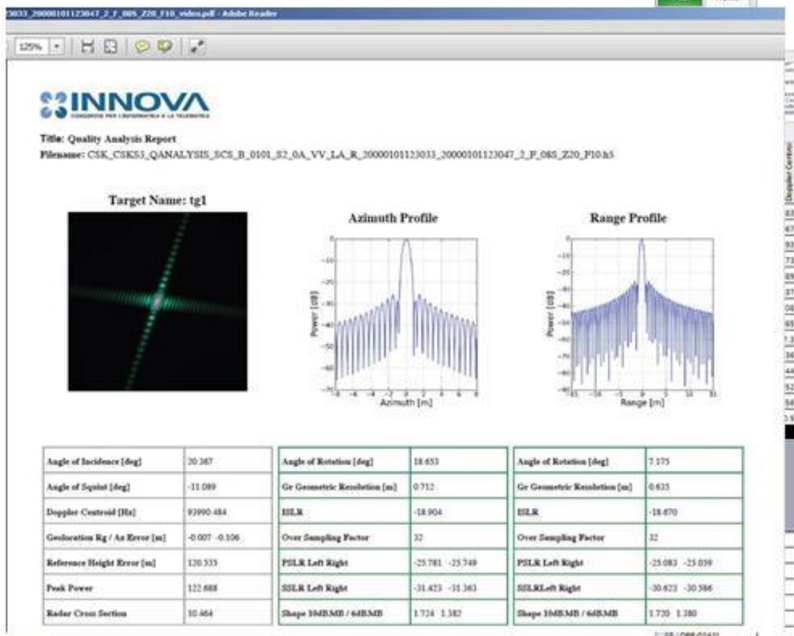

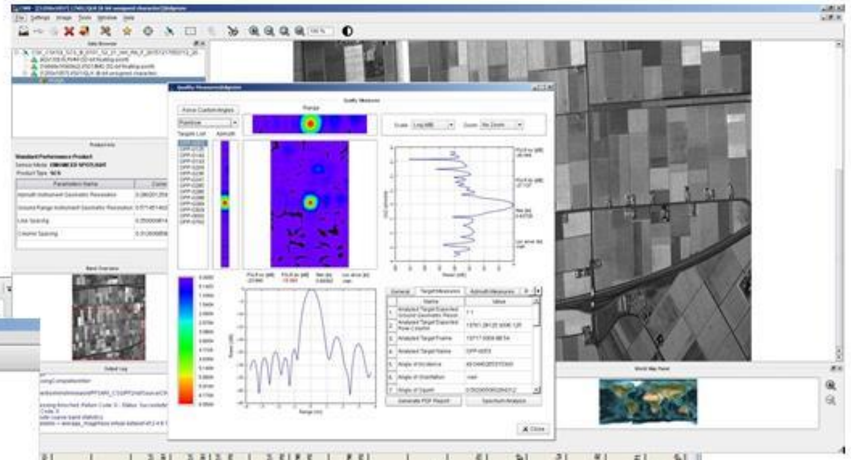

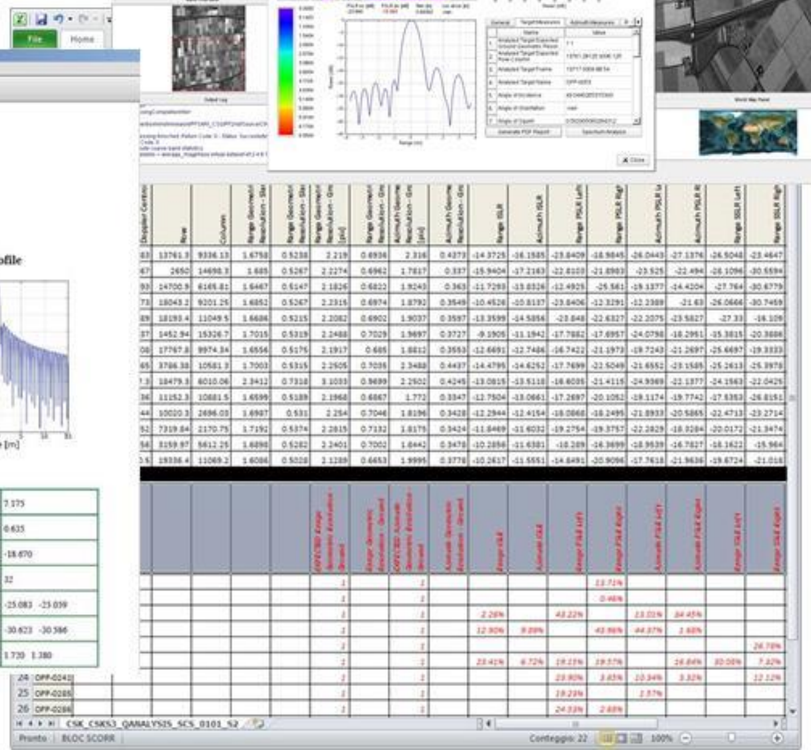

Presentation Index:

- Introduction
- Algorithms Description
- Architecture Overview
- Dataset Description
- Performances Analysis and Benchmarks
- Conclusions
- Acknowledgments

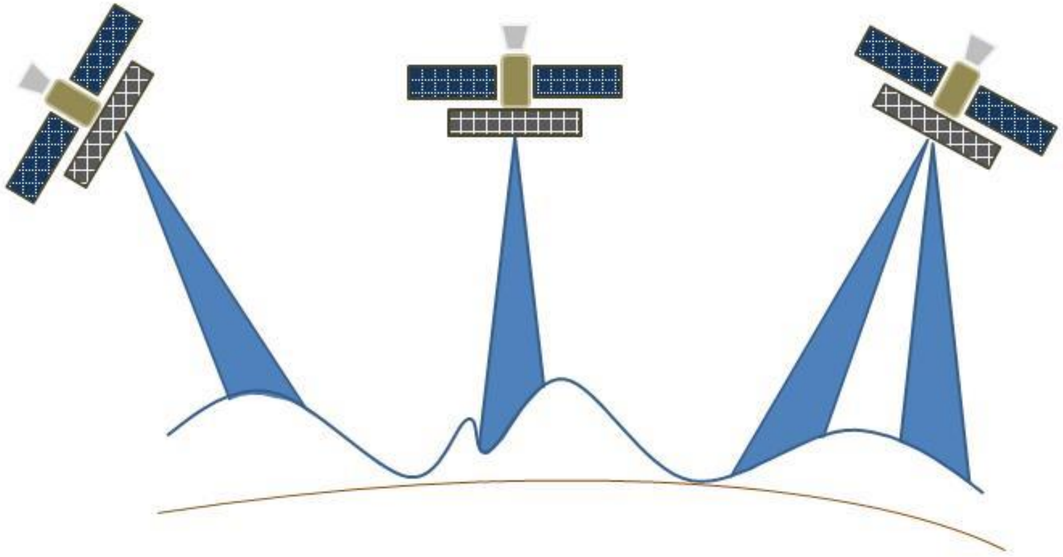

Challenging scenario of new upcoming satellite SAR missions:

- **Ultra-high resolution Spotlight** acquisitions performed exploiting long integration time
- Very high satellite agility to acquire wider areas with finer resolutions even in near-contiguous frames within a reduced time period which means the need to have Spotlight **high squinted acquisition** geometry
- The need to perform acquisition globally and on the areas with **strong topography variations**.

➔ **This characteristics could result in a significant degradation of the SAR data focusing performance, mostly for the algorithms working in the Fourier-domain**

➔ **New accurate and efficient Spotlight image formation algorithm that uses a focusing core implemented in the time-domain**

Frequency domain focusing concept

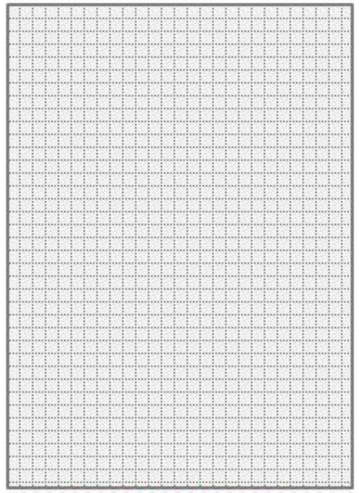

Input RAW data f_{in}

$$f_{in}(t_{az}, t_{rg}) \overset{FFT}{\Longrightarrow} F(X,Y)$$

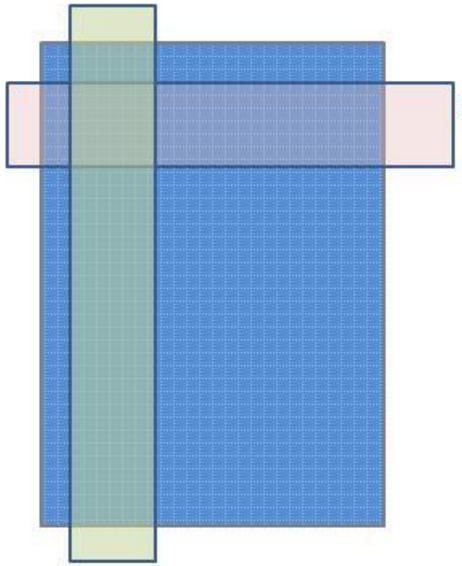

Frequency domain operations

Frequency domain operations

$$F'(X,Y) \overset{FFT^{-1}}{\Longrightarrow} f_{out}(t_{row}, t_{col})$$

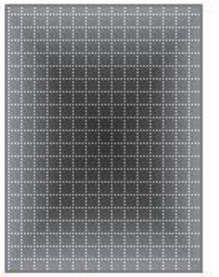

Output Image f_{out}

Time domain focusing concept

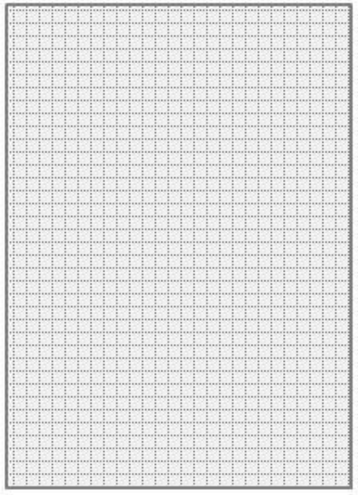

Input RAW data f_{in}

$$f_{out}(t_{row}, t_{col}) = f(t_{az}, t_{rg}) * h_{row,col}(t_{az}, t_{rg})$$

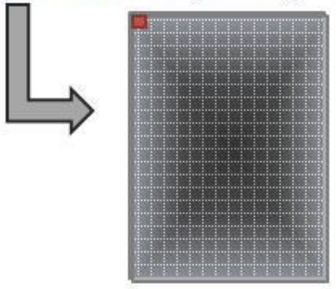

$(\cdots)$

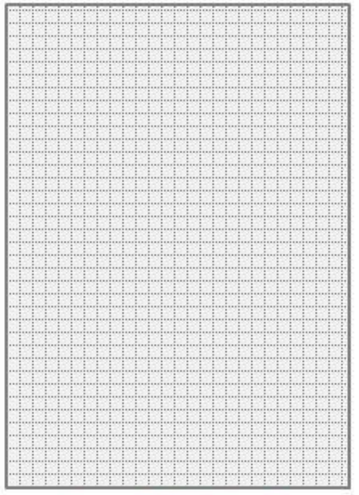

Input RAW data f_{in}

$$f_{out}(t_{row}, t_{col}) = f(t_{az}, t_{rg}) * h_{row,col}(t_{az}, t_{rg})$$

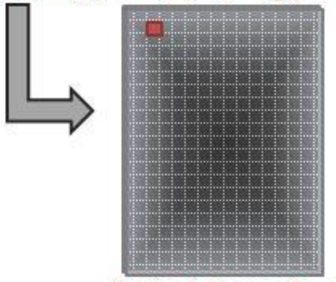

Output Image f_{out}

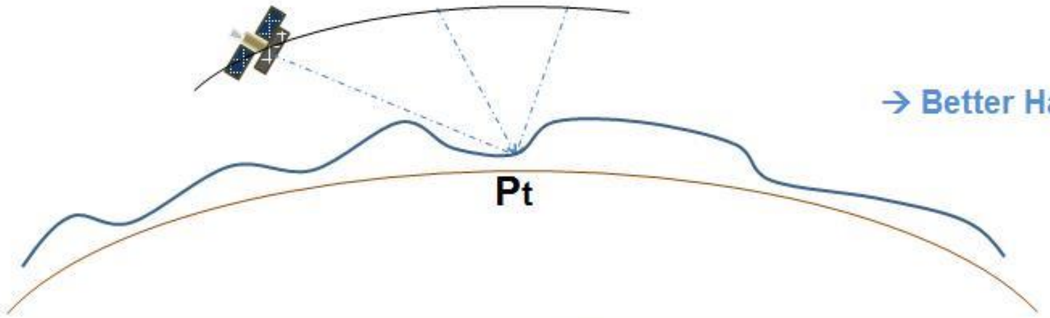

→ Better Handling of Local Topography Variation

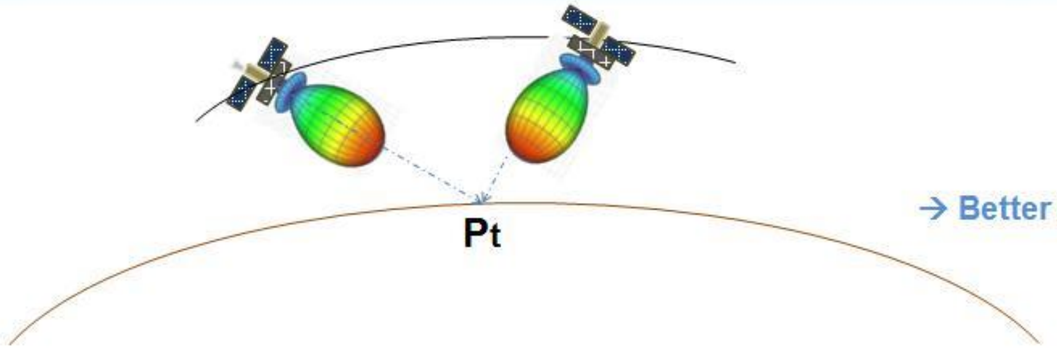

→ Better compensation of 3D Antenna Pattern

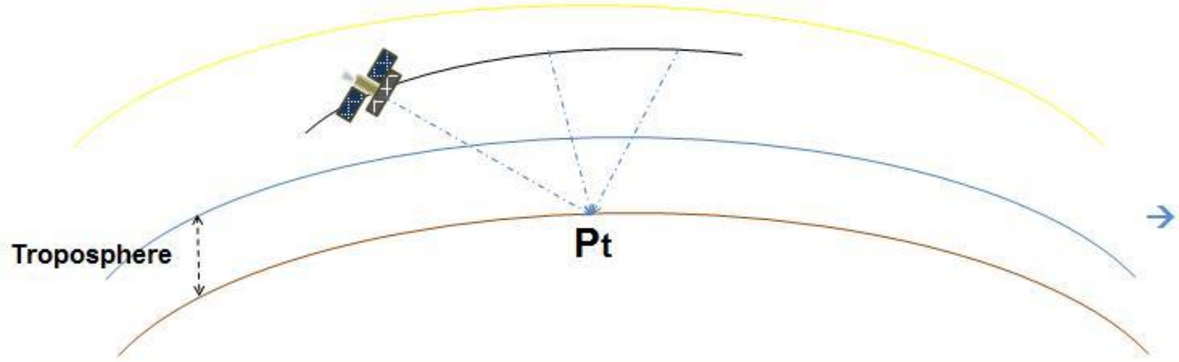

→ Better Point By Point Ray By Ray Atmospheric Effects Compensation

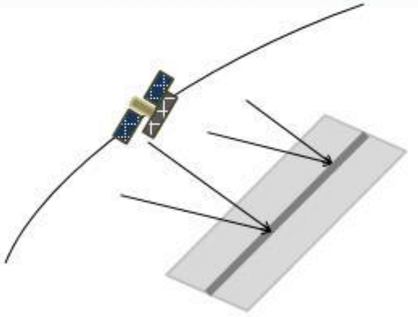

→ Better Compensation of Bistatic Effects

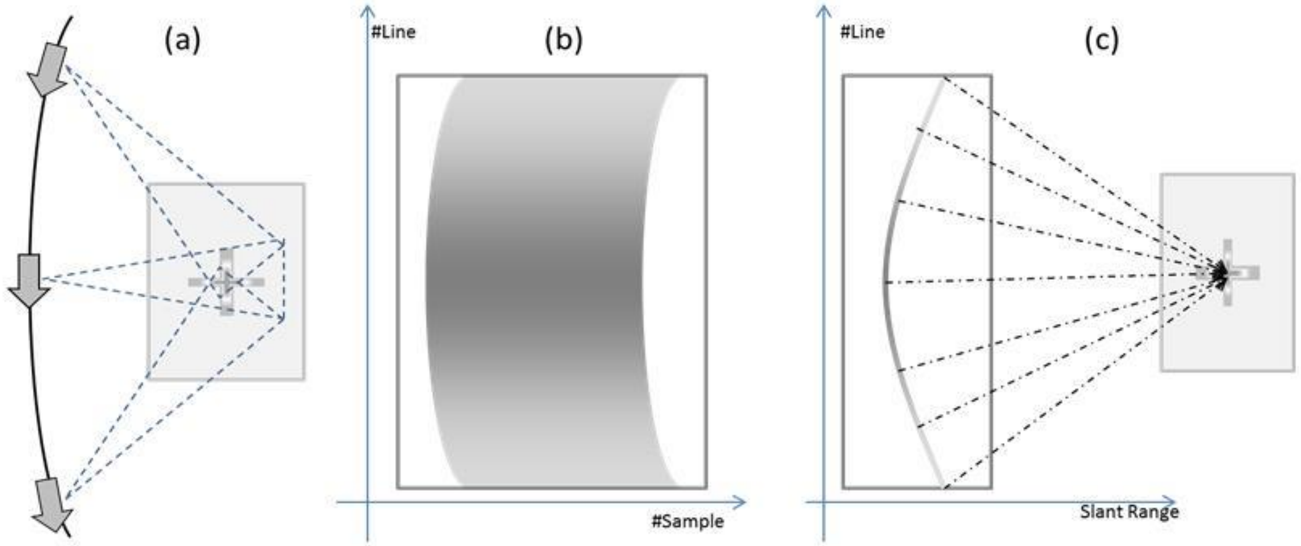

Pictorial representation of a spotlight acquisition over an area with a single point target:

(a) The target falls into the antenna beam for each acquired echo lines
(b) The grey area represents all the samples of input RAW data for which the energy of a single pixel of output image it is spread.
(c) After the range compression it is necessary to back project the target energy on its correct position and this energy is present in all the image lines.

→ Great advantages of TDBP algorithm it is the possibility to adapt the characteristics of the focusing transfer faction on a pixel bases to obtain optimal focusing performances on all the scene regardless on local height or local squint angle.

→ **Main drawbacks of using the TDBP algorithms is the great computational burden due to the need to use almost all the input data samples to focus each pixel of output image.**

The mathematical **model** behind the Time Domain Back Projection focusing method, one of the first focusing algorithms described in literature, is very simple. Considering that the proposed solution starts from range-compressed data, the formula used to reconstruct each of the pixels of the output image is:

$$I(x,y) = \int_{t_a \epsilon L} K(t_a,x,y) \cdot g\big(t_a, r(t_a,x,y)\big) \cdot e^{-j\frac{4\cdot\pi}{\lambda}\cdot r(t_a,x,y)} \cdot dt_a$$

This reveals some important characteristics of this imaging approach: the focusing of each pixel require to use samples from all the lines of input RAW data but it is also independent from the focusing of the other pixels of the output image.

The first characteristic is the reason of the **high computational cost** of the algorithm while the second characteristic suggest that it is possible to reach an **high degree of parallelism** using the TDBP processing approach.

Reducing the number of the output pixels to be generated or reducing the number of input echo lines to be used to focus each of the output pixels it is a good strategy to reduce the overall computational complexity of the back-projection algorithm.

In order to use the time domain focusing in an operational scenario it is necessary to introduce algorithm optimizations to reduce the overall computational coast without introducing significant degradation in the focusing quality.

The proposed solution is based on the use of a **sub-apertures processing approach**.

For the standard processing chain the $N^{BP}_{STANDARD}$ represents the number of operations required to obtain all the pixels of the output products; when sub-apertures technique is used, this number is N^{BP}_{SUBA} and it is reduced by a computational gain factor *D* respect to the standard case. *D* is a factor strongly related to the number of sub-apertures used.

- Focusing each of the N^{SUBA} sub-apertures with TDBP algorithm means to use a reduced number of input echo lines for each sub aperture.
- Lower resolution of each focused sub-aperture allows for larger spacing and thus to have fewer output pixels with the same coverage.
- Each focused sub-aperture must be accumulated in the final product output grid after oversampling along the rows direction.

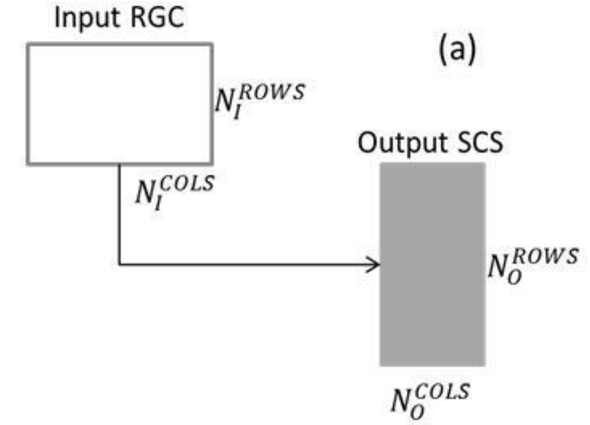

$$N^{BP}_{STANDARD} = \left(\left(N_O^{ROWS} \cdot N_O^{COLS} \right) \cdot N_I^{ROWS} \right)$$

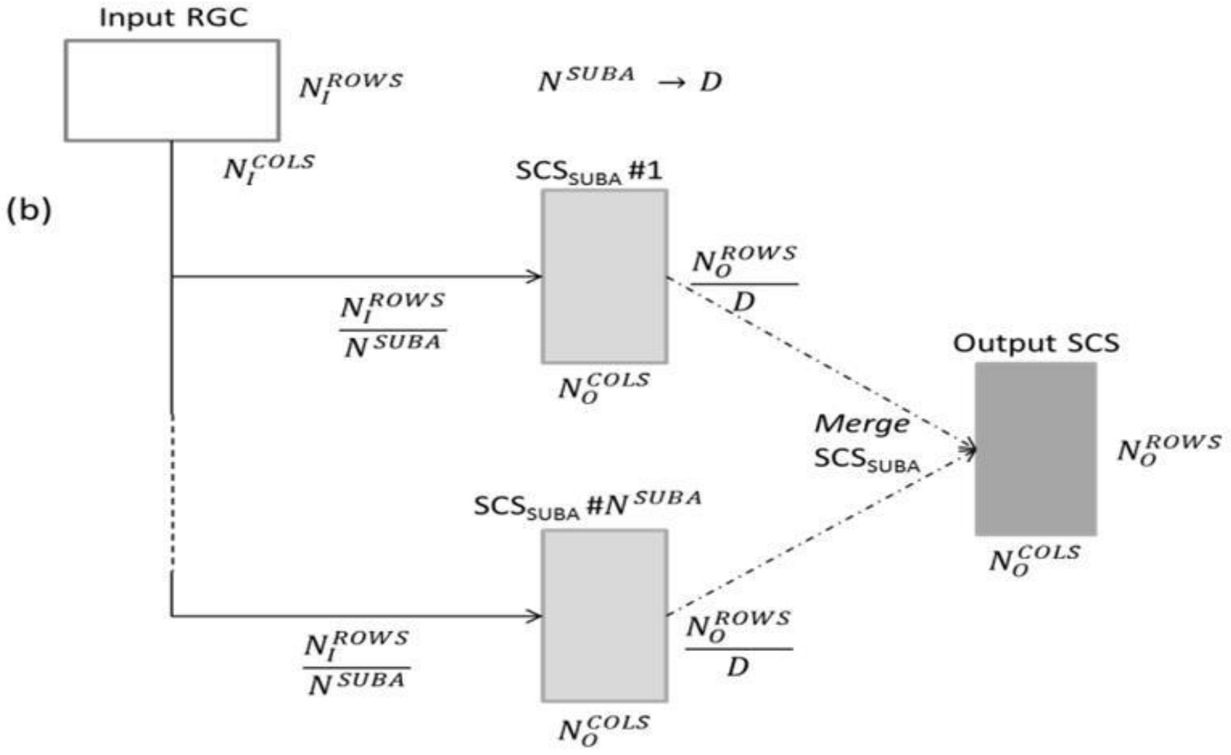

$$N^{BP}_{SUBA} = \left(\left(\frac{N_O^{ROWS}}{D} \cdot N_O^{COLS} \right) \cdot \frac{N_I^{ROWS}}{N^{SUBA}} \right) \cdot N^{SUBA} = \frac{N^{BP}_{STANDARD}}{\boldsymbol{D}}$$

The Nyquist requirements must be met and for low resolution images and for this reason gain factor D although closely related to the number of sub-apertures is not exactly equal to it due to the effects introduced by steering and squint of the signal at very high resolution as shown in the next figures.

From this consideration it is clear that the maximum computational gain obtainable is not indeterminate but tends to saturate as the number of sub-apertures increases. The choice of the optimum number of sub-apertures to be used depends on the characteristics of the data to be focused.

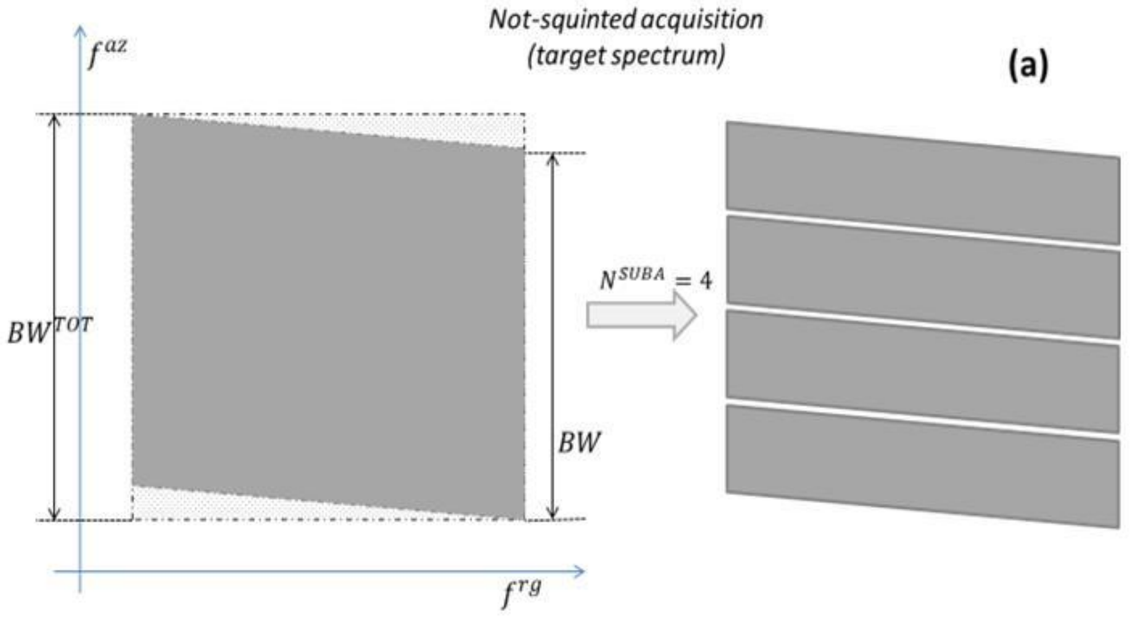

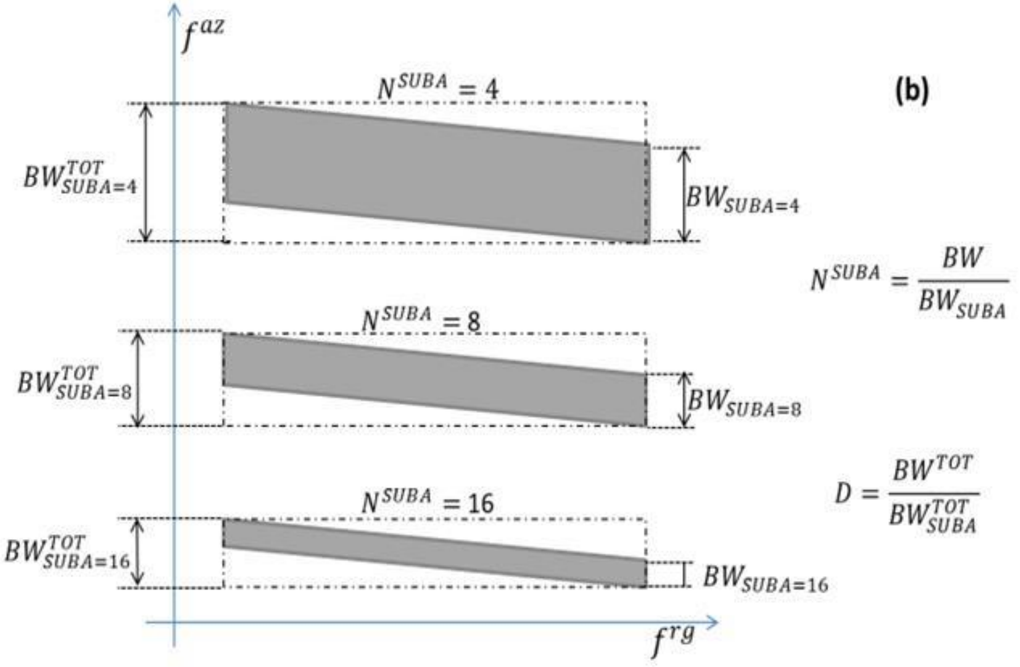

For the **squinted acquisitions** the presence of the squint and the rotation of the target spectrum increase the difference between the total bandwidth and the target bandwidth; this minimizes the gain obtainable through the sub-apertures processing optimization technique.

The solution to this limitation is to process the entire band of the target divided into a set of non-overlapping range-looks, this allows to greatly reduce the value of the difference between $(BW_{SUBA}^{TOT} - BW_{SUBA})$ and consequently to strongly increase the value of the computational gain obtainable with the sub-apertures processing.

The figure on the right shows that after merging the contribution of all the sub-apertures, the portions of the spectrum for each range-look must also be recomposed to obtain the completed spectrum of the target.

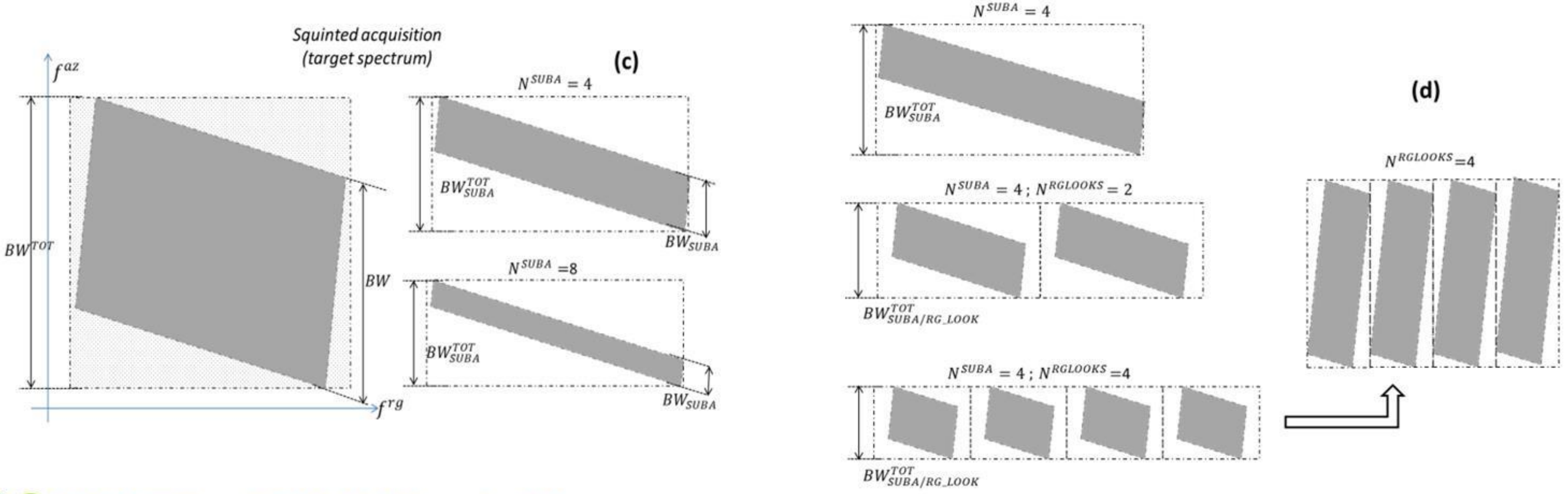

In the case of **very high resolution squinted** acquisition a different optimization solution based on the use of sub-apertures applied to separated range-looks needs to be implemented.
The $N^{BP}_{SUBA\ \&\ RGLOOKS}$ is reduced by a computational gain factor *D* respect to the standard case of TDBP processing without any optimization and multiplied by the ratio $\frac{N^{RGLOOKS}}{R}$. The computational gain D is much greater than the one obtainable without the use of range looks optimization for the squinted acquisitions. The $\frac{N^{RGLOOKS}}{R}$ ratio is about 1 for low $N^{RGLOOKS}$ values and it assumes values much greater than 1, as the number of range-looks increases.

- A certain number of non overlapped range-looks have to be extracted from the input RGC image and processed using the TDBP algorithm with sub-apertures optimization.
- Each focused range look must be accumulated in the output product grid after oversampling in the columns direction.

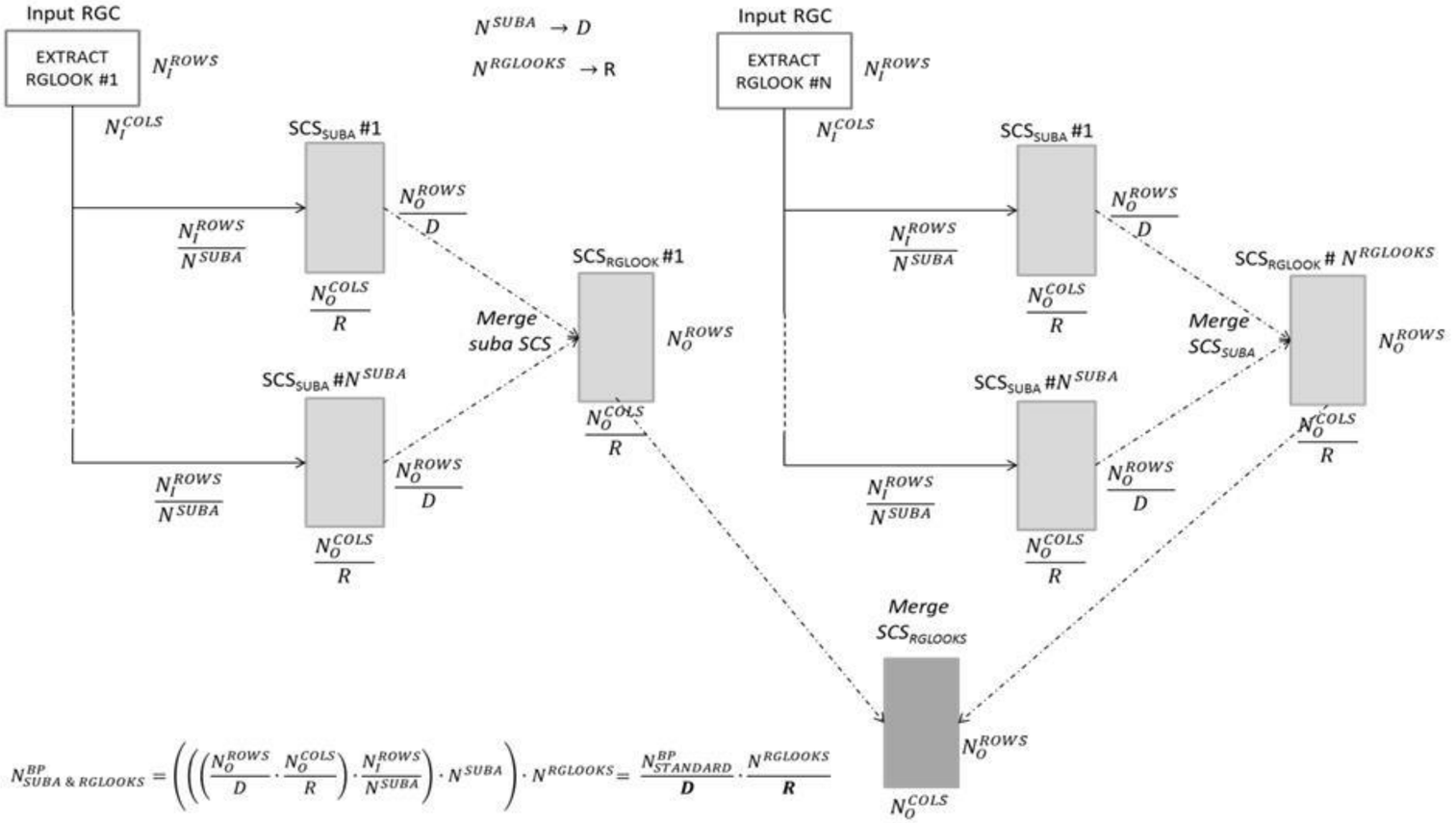

STANDARD processing chain with Time Domain Back projection focusing without optimizations

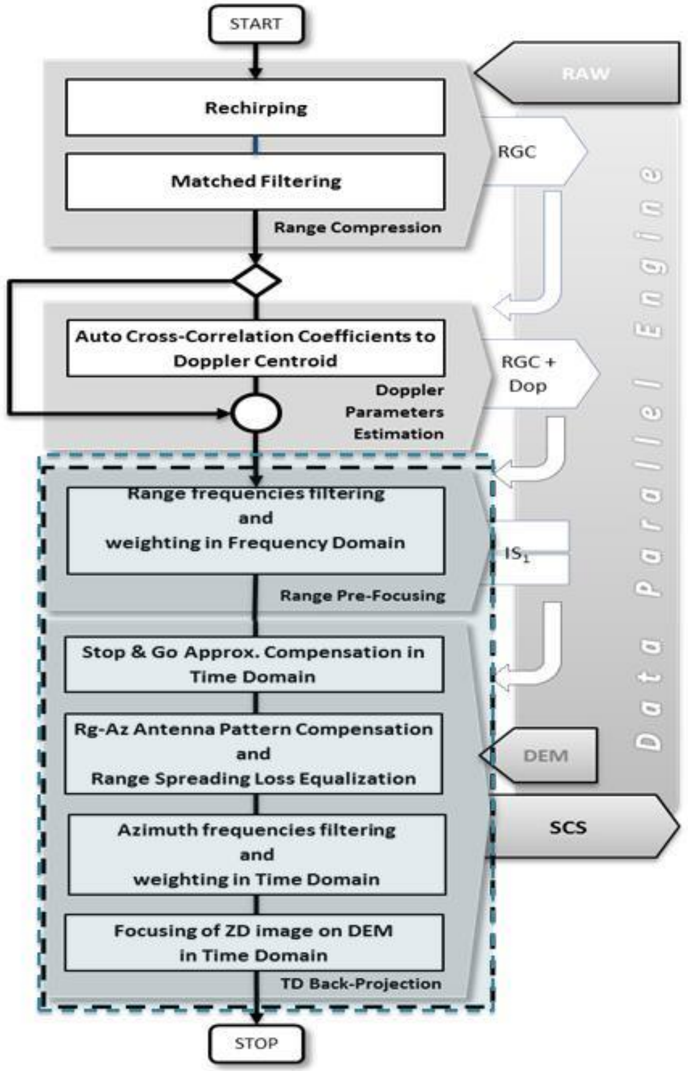

1. Range Compression
2. Doppler Parameter Estimation
3. Range Pre-Focusing
4. Focusing with TD Back-Projection

Each of the above steps is performed by cloning the algorithm in different instances that operate parallel to generate a well defined portion of the output (Data-parallel or Embarrassingly-parallel computation), either intermediate (RGC, IS1) or final (SCS).

Intermediate images are kept in memory, stored on disk only if necessary.

The pre-focusing range phase prepares the range-compressed image by structuring it in such a way that it can be accessed efficiently by dozens or hundreds of parallel processes (threads) used for focusing through TD Back-Projection.

FAST processing chain with Time Domain Back projection focusing with sub-apertures optimization

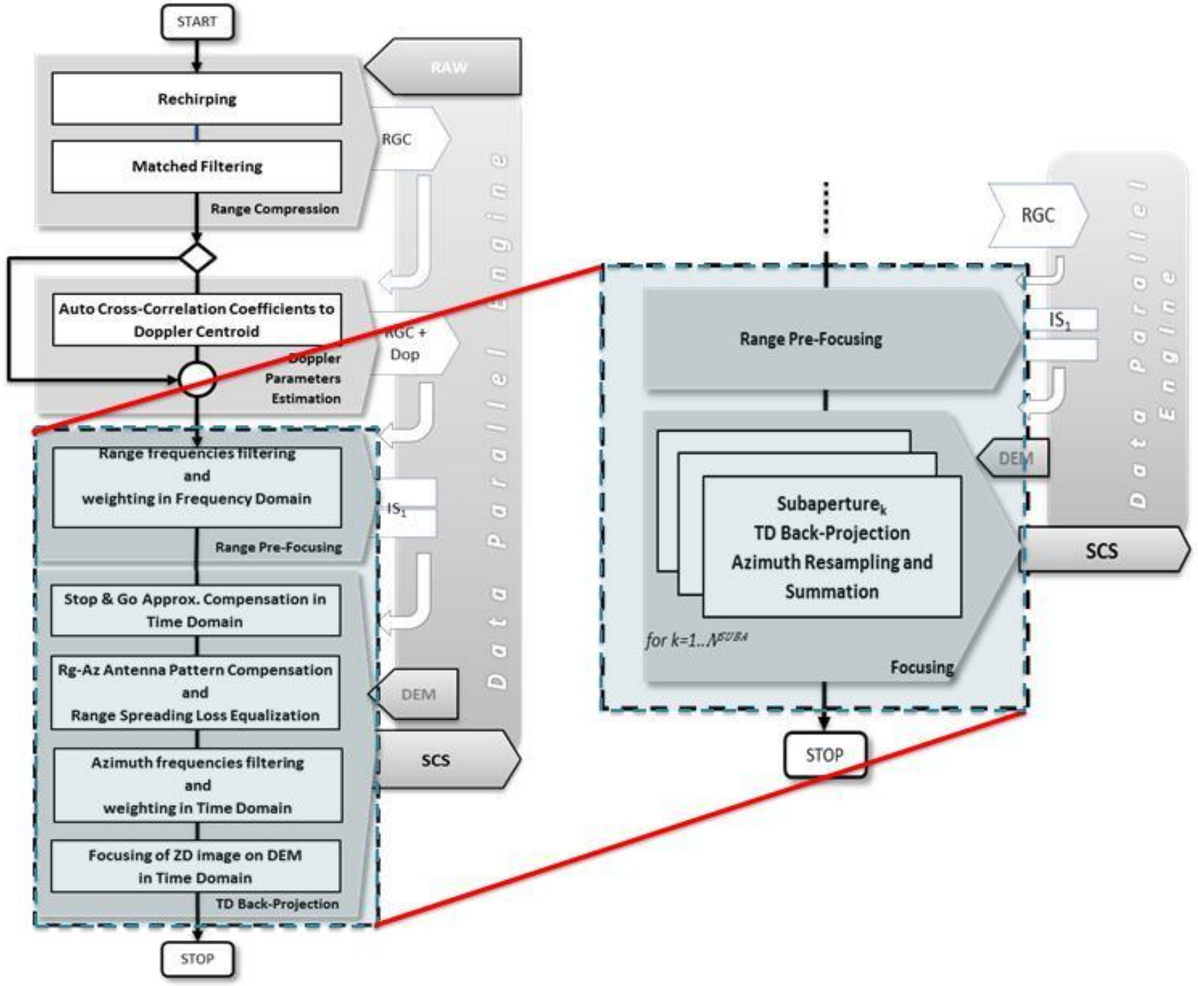

1. Range Compression
2. Doppler Parameter Estimation
3. Range Pre-Focusing
4. Focusing with TD Back-Projection with sub-apertures approach.

FAST processing chain with Time Domain Back projection focusing with sub-apertures and range-looks optimizations

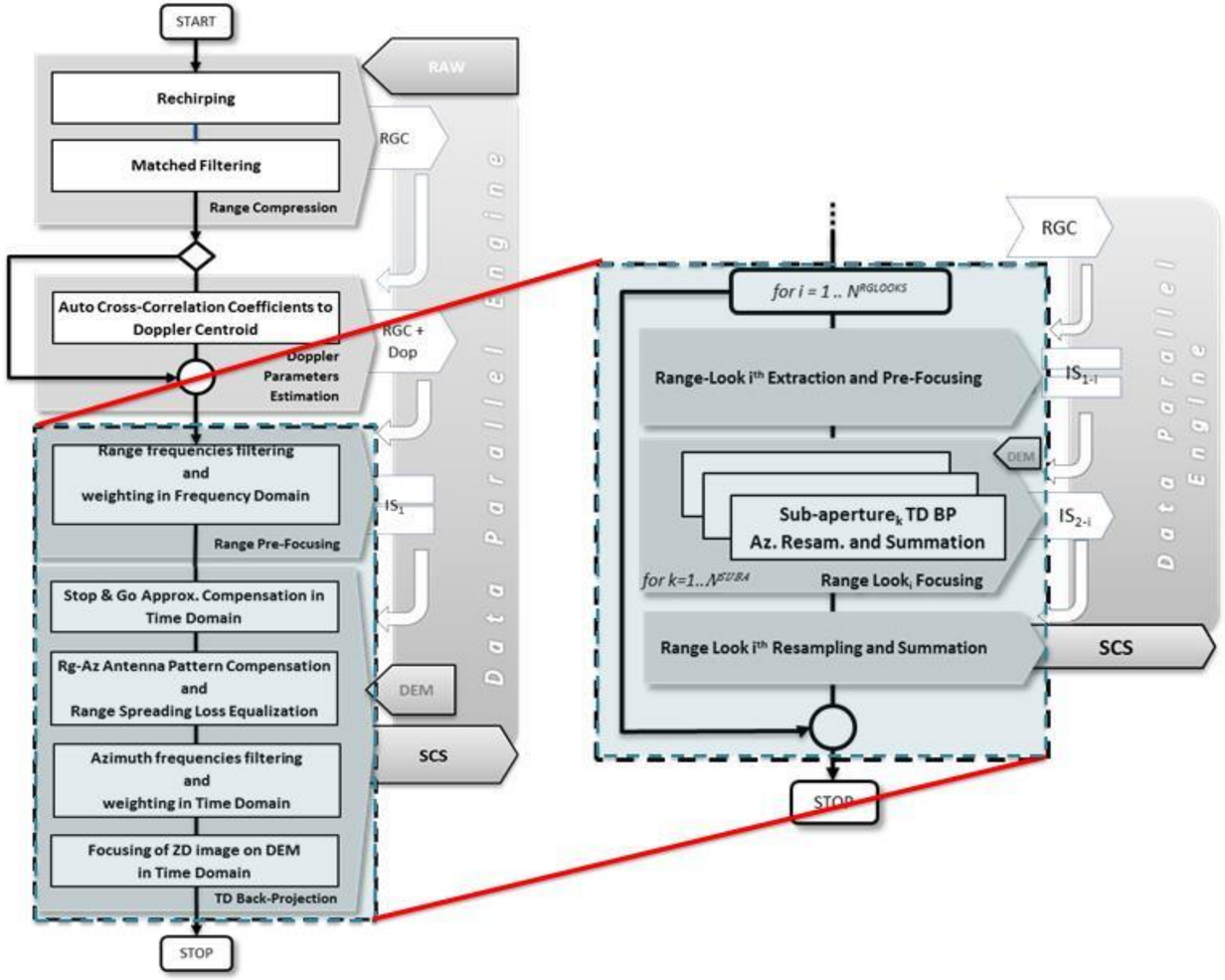

1. Range Compression
2. Doppler Parameter Estimation
3. Range Pre-Focusing
4. For i=1 to $N^{RGLOOKS}$ do
   a) Range Look i-th: Extraction and Pre-Focusing
   b) Range Look i-th: Focusing with TDBP with sub-apertures
   c) Range Look i-th: oversampling and accumulation in the output SCS grid.

Test Dataset

Mode ID and Geometry[7]	ID	Squint Angle at scene centre [deg]	Incidence Angle at scene centre [deg]	Spatial Coverage Rg x Az [km]	Geometric Resolution at scene centre[2] Rg x Az [m]	Chirp Bandwidth [MHz]	Doppler Bandwidth 3dB [KHz]	Scene Topography
S2A-Plus[1] Sliding	(af)	12°	24.223°	8 x 3.4	0.483 x 0.364	919	22.5	FLAT
	(a)	12°	23.992°	8 x 3.4	0.483 x 0.364	919	22.5	INCLINED PLANE[3,4]
S2B-Plus[1] Sliding	(b0)	0°	24.286°	11 x 11	0.484 x 0.567	792	12.9	INCLINED PLANE[3,5]
	(bf)	12°	20.216°	11 x 11	0.562 x 0.662	797	12.6	FLAT
	(b)	12°	23.875°	11 x 11	0.556 x 0.656	797	12.6	INCLINED PLANE[3,5]
UUHR Staring	(u0f)	0°	34.269°	3 x 3	0.119 x 0.105	2397	71.1	FLAT
	(u)	12°	34.161°	3 x 3	0.117 x 0.117	2397	65.8	INCLINED PLANE[3,6]

[1] Stress tests under extreme acquisition conditions w.r.t. S2A and S2B in [1].
[2] The ground geometric resolution values is related to the output of a weighting Hamming filter with α=0.68.
[3] This topography configuration was chosen for convenience reasons. The algorithm works on any configuration through the use of DEM.
[4] From 0m at Near Edge to 2000m at Far Edge; [5]From 0m at Near Edge to 3000m at Far Edge; [6]From 0m at Near Edge to 1500m at Far Edge
[7] STARING those acquisitions in which the antenna rotation center lies exactly on the ellipsoid surface during the acquisition phase (antenna steering); SLIDING the acquisitions in which the rotation center is positioned below the ellipsoid surface.

[1] "COSMO-SkyMed di Seconda Generazione SAR image focusing of spotlight data for civilian users" - SPIE Image and Signal Processing for Remote Sensing 2018

Main characteristics the raw data simulator:

- Complete and accurate radar parameters control (Carrier Frequency, PRF, Sampling Rate, Chirp Bandwidth, Chirp Duration)
- Accurate earth model
- Accurate geometric constraints definition (look side, orbit direction, incidence angle)
- Coherent orbital and attitude parameters
- Accurate definition of electronic steering model, range and azimuth coverages, azimuth resolution.
- Accurate antenna beam features definition.
- **Non-validity of the start/stop approximation**
- Complete scene control options (number of targets and their arrangement, backscattering coefficient, **scene topography, tropospheric path delay**)

Dataset Details: dimensions and sizes of input RAW data, output of range compression and output SCS files

Mode ID Geometry [1]	ID	RAW UINT8			Range Compressed (IS_1) FLOAT32			Complex Focused Image (SCS) FLOAT32		
		#Rows	#Cols	Size MB	#Rows	#Cols	Size MB	#Rows	#Cols	Size MB
S2A-Plus Sliding	(af)	36966	28000	1975	36966	144000	40613	21294	20736	3369
	(a)	36966	28000	1975	36966	144000	40613	21294	20580	3344
S2B-Plus Sliding	(b0)	38986	35000	2603	38986	41067	12215	28224	28350	6105
	(bf)	45046	35000	3008	45046	147000	50521	44000	24948	8375
	(b)	45046	35000	3008	45046	147000	50521	44000	24948	8375
UUHR Staring	(u0f)	50500	48000	4624	50500	85995	33133	37500	32000	9156
	(u)	50500	48000	4624	50500	494208	190411	50000	32000	12208
CSK S2 Sliding	ES-16	25296	24832	1199	25296	19712	3804	15840	18720	2263

[1] *STARING those acquisitions in which the antenna rotation center lies exactly on the ellipsoid surface during the acquisition phase (antenna steering); SLIDING the acquisitions in which the rotation center is positioned below the ellipsoid surface.*

This information has been considered during the design of the software prototype and the choice of the HW test platform to ensure that the processing steps, operating in data parallel mode, could efficiently handle the huge amount of image data without encountering problems in memory usage

Main characteristics the simulation process:

The simulation process includes orbital data generation, attitude and electronic pointing management, two-dimensional beam radiation diagram forming, target arrangement into the observed scene and finally the signal simulation, performed in the time domain target by target, on the basis of the superposition effects into the output complex raster layer, including signal deramping in the case of Spotlight mode.
Finally, the product is formatted with the requested output data quantization and metadata evaluation.

The layout used for all the data presents in the dataset includes nine point targets arranged on a 3 x 3 grid, it is suitable for supporting most of the algorithmic analysis and image quality assessment phases

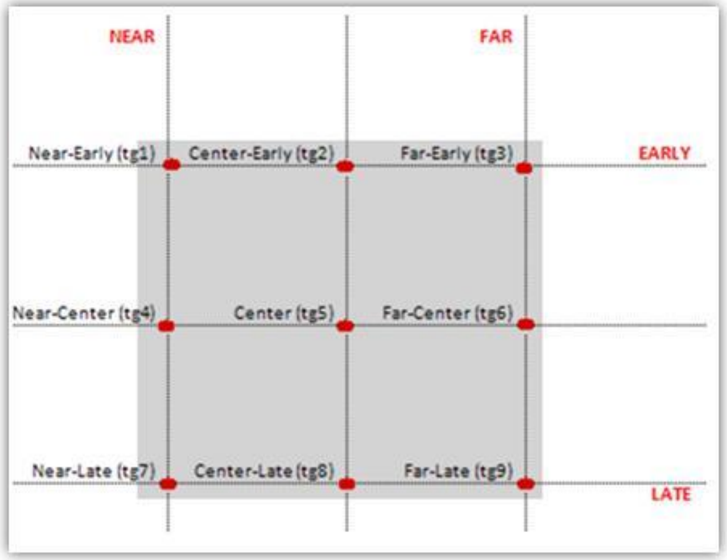

Dataset Description

IRF performance and Processing Time performances obtained with the optimized TDBP algorithm considering very challenging data where are simultaneously present:

- **very and ultra high resolutions;**
- **high squints angles;**
- **high coverages;**
- **strong variations of the targets height in the scene.**

Total processing time, measured on a reference high-performance hardware platform, typical of an operational environment, with the following features:
4 Intel® Xeon® Platinum 8176 CPU 28C / 56T 38.5MB L3 @ 2.10 GHz / 3.80GHz - 384 GB RAM.
All the processes were carried out using a support DEM.

# Range Looks - # Subapertures			2 - 8	4 - 34	6 - 72	8 - 66
TDBP Computational Gain			3.82	7.95	10.97	11.93
(a) S2A-Plus 12° 0÷2000 m						
Standard TDBP Total Processing time 13h 7' = 787.2'	-40 [dB] -30 -25 -3	Far-Early #3	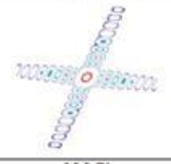			
Total Processing Time			225.7'	114.9'	95.3'	93.3'=1h33'18''
Speed-up Factor			3.49	6.85	8.26	8.44

(a) S2A-Plus 12° squint, 8 x 3.4 Km, Height 0÷2000m

(a) Far-Early target #3		Range Resolution	Azimuth Resolution	Range PSLR	Azimuth PSLR	Range Shape 6dB/3dB	Range Shape 10dB/3dB	Azimuth Shape 6dB/3dB	Azimuth Shape 10dB/3dB	Ground Range Geolocation Error [m]	Azimuth Geolocation Error [m]
#Range Looks	#Subapertures										
Standard		0.467	0.365	-25.04	-25.25	1.380	1.720	1.381	1.722	-0.001	0.000
2	8	0.467	0.365	-25.24	-25.36	1.380	1.720	1.381	1.722	-0.002	0.001
4	34	0.467	0.365	-24.97	-25.18	1.380	1.720	1.381	1.722	-0.002	0.000
6	72	0.466	0.366	-25.01	-25.15	1.380	1.720	1.381	1.722	-0.003	0.000
8	66	0.469	0.367	-24.93	-25.64	1.380	1.720	1.381	1.722	0.000	0.001

Processing Parameters		Total Processing Time
#Rg Looks	#Sub-apertures	
STANDARD		**13h 7'**
2	8	3h 46'
4	34	1h 55'
6	72	1h 36'
8	66	**1h 33'**

(b) S2B-Plus 12° squint, 10 x 10 Km, Height 0÷3000m

# Range Looks - # Subapertures	2 - 18	4 – 34	6 - 50	8 - 66
TDBP Computational Gain	4	7.2	9.5	11.34
(b) S2B-Plus 12° 0÷3000 m	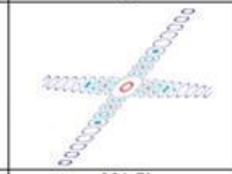			
Standard TDBP Total Processing time 1103' = 18h 23''				
Total Processing Time	291.7'	180.5'	156.7'	145.6'=2h25'36''
Speed-up Factor	3.78	6.11	7.04	7.58

(b) Far-Early target #3		Range Resolution	Azimuth Resolution	Range PSLR	Azimuth PSLR	Range Shape 6dB/3dB	Range Shape 10dB/3dB	Azimuth Shape 6dB/3dB	Azimuth Shape 10dB/3dB	Ground Range Geolocation Error [m]	Azimuth Geolocation Error [m]
#Range Looks	#Subapertures										
Standard		0.532	0.666	-25.08	-25.18	1.380	1.720	1.381	1.722	-0.002	0.002
2	18	0.532	0.667	-25.07	-25.17	1.380	1.720	1.381	1.722	-0.002	0.002
4	34	0.533	0.666	-25.00	-25.13	1.380	1.720	1.381	1.722	-0.001	0.001
6	50	0.533	0.666	-25.00	-25.13	1.380	1.720	1.381	1.722	0.000	0.001
8	66	0.532	0.666	-25.03	-25.20	1.380	1.720	1.381	1.722	0.000	0.001

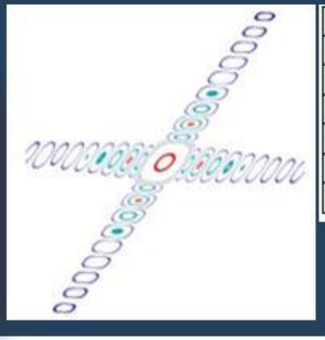

Processing Parameters		Total Processing Time
#Rg Looks	#Sub-apertures	
STANDARD		18h 23'
2	18	4h 52'
4	34	3h 01'
6	50	2h 37'
8	66	2h 25'

(u) UUHR 12° squint, 3 x 3 km, Height 0÷1500m

# Range Looks - # Subapertures	2 - 22	4 - 42	6 - 64	8 - 58
Computational Gain	5.5	9	11.31	12
(u) UUHR 12° 0÷1500m	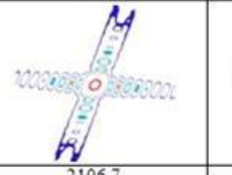			
Standard TDBP Total Processing time 9257.3' = 6d10h17'11''				
Total Processing Time	2106.7'	1173.8'	920.9'	907.9'=15h7'41''
Speed-up Factor	4.39	7.89	10.06	10.20

(u) Near-Late target #7		Range Resolution	Azimuth Resolution	Range PSLR	Azimuth PSLR	Range Shape 6dB/3dB	Range Shape 10dB/3dB	Azimuth Shape 6dB/3dB	Azimuth Shape 10dB/3dB	Ground Range Geolocation Error [m]	Azimuth Geolocation Error [m]
#Range Looks	#Subapertures										
Standard		0.115	0.118	-25.13	-26.16	1.381	1.721	1.381	1.723	0.000	0.000
2	22	0.115	0.118	-25.07	-26.08	1.381	1.721	1.381	1.723	0.000	0.000
4	42	0.115	0.118	-25.12	-26.10	1.381	1.721	1.381	1.723	0.001	0.000
6	64	0.115	0.118	-25.12	-25.96	1.381	1.721	1.381	1.723	0.000	0.000
8	58	0.115	0.118	-25.03	-25.99	1.381	1.721	1.381	1.723	-0.001	0.001

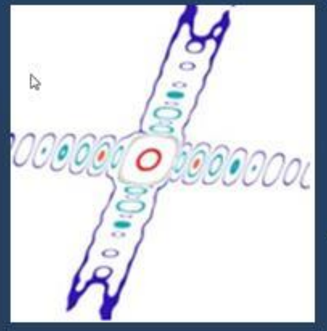

Processing Parameters		Total Processing Time
#Rg Looks	#Sub-apertures	
STANDARD		6d 10h 17'
2	22	1d 11h 6'
4	34	19h 33'
6	50	15h 21'
8	66	15h 07'

Comparison of IRF performances between the TDBP algorithm and a standard focus algorithm in the frequency domain based on Omega-K core for a high-resolution high squinted data with a large coverage on the ground.

(bf) S2B-Plus 12° Flat				Time Domain Back Projection			Frequency Domain Ω-K		
				Contour Plot and Doppler history	Geolocation performance		Contour Plot and Doppler history	Geolocation performance and resolution loss %	
-40 (dB) -30 -25 -3	Far-Early #3	Height [m]	0	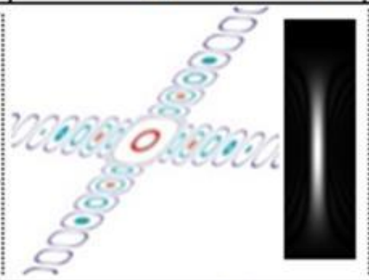	Ground Range Geolocation Error [m]	0.000	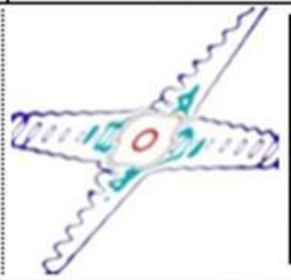	Ground Range Geolocation Error [m]	0.345
		Angle of Incidence [deg]	21.20		Azimuth Geolocation Error [m]	0.001		Azimuth Geolocation Error [m]	-0.909
		Angle of Squint [deg]	-13.74					Ground Range Resolution loss	6.42%
								Azimuth Resolution loss	15.6%
	Center #5	Height [m]	0	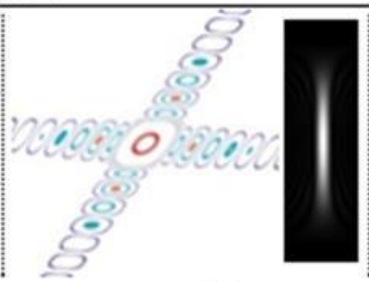	Ground Range Geolocation Error [m]	0.000	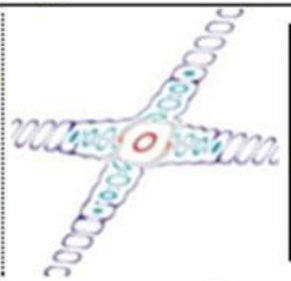	Ground Range Geolocation Error [m]	0.177
		Angle of Incidence [deg]	20.72		Azimuth Geolocation Error [m]	0.001		Azimuth Geolocation Error [m]	-0.315
		Angle of Squint [deg]	-11.58					Ground Range Resolution loss	1.92%
								Azimuth Resolution loss	0%
	Near-Late #7	Height [m]	0	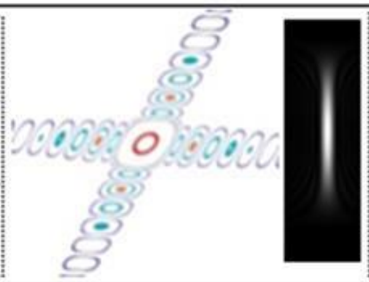	Ground Range Geolocation Error [m]	-0.002	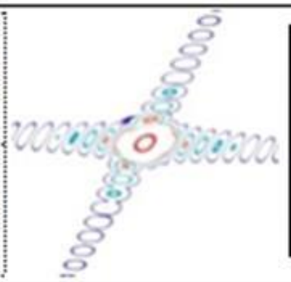	Ground Range Geolocation Error [m]	1.478
		Angle of Incidence [deg]	20.21		Azimuth Geolocation Error [m]	0.001		Azimuth Geolocation Error [m]	-3.777
		Angle of Squint [deg]	-9.42					Ground Range Resolution loss	1.90%
								Azimuth Resolution loss	0%

Comparison of IRF performances between the TDBP algorithm and a standard focus algorithm in the frequency domain based on Omega-K core for a ultra high-resolution data.

(u0f) UUHR 0° Flat				Time Domain Back Projection			Frequency Domain Ω-K		
				Contour Plot	Geolocation performance		Contour Plot	Geolocation performance and resolution loss %	
[dB] -40 -30 -25 -3	Far-Early #3	Height [m]	0	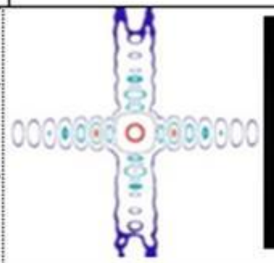	Ground Range Geolocation Error [m]	0.001		Ground Range Geolocation Error [m]	-0.001
		Angle of Incidence [deg]	34.38		Azimuth Geolocation Error [m]	0.000		Azimuth Geolocation Error [m]	0.002
		Angle of Squint [deg]	0.12					Ground Range Resolution loss	2.50%
								Azimuth Resolution loss	3.27%
	Center #5	Height [m]	0	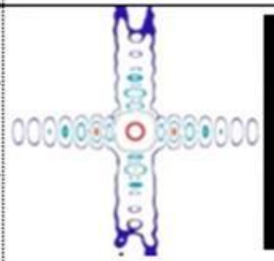	Ground Range Geolocation Error [m]	0.000	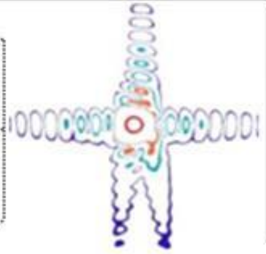	Ground Range Geolocation Error [m]	0.004
		Angle of Incidence [deg]	34.27		Azimuth Geolocation Error [m]	0.000		Azimuth Geolocation Error [m]	-0.005
		Angle of Squint [deg]	0					Ground Range Resolution loss	3.26%
								Azimuth Resolution loss	4.69%
	Near-Late #7	Height [m]	0	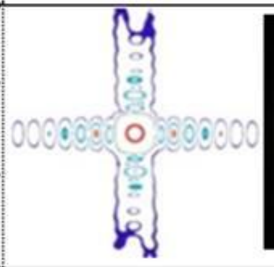	Ground Range Geolocation Error [m]	0.000	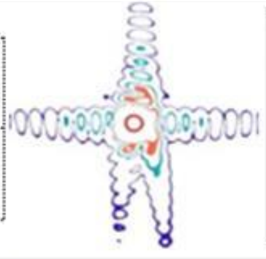	Ground Range Geolocation Error [m]	0.009
		Angle of Incidence [deg]	34.16		Azimuth Geolocation Error [m]	0.000		Azimuth Geolocation Error [m]	-0.003
		Angle of Squint [deg]	-0.12					Ground Range Resolution loss	3.98%
								Azimuth Resolution loss	5.94%

Results obtained focusing a high resolution real image using the TDBP processing algorithm.

(CSK-S2) COSMO-SkyMED Enhanced Spotlight on Rosamond Lake Area.

Corner Reflector Array (RCRA)
Rosamond Dry Lake Bed,
California, USA
(uavsar.jpl.nasa.gov)

(a)

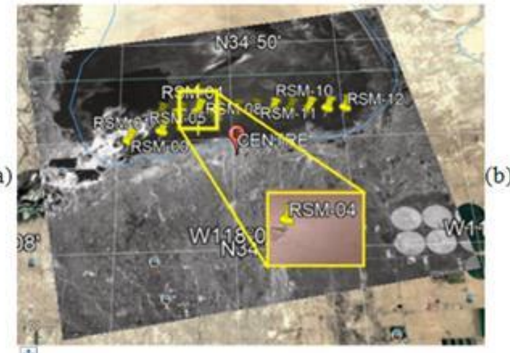

(b)

# Range Looks- # Subapertures		1 – 1	1-64	2-32
TDBP Computational Gain		-	22	24
COSMO SkyMED SAR4 ES-16 HH Center Squint [deg]: 0.107 Coverage [Km] 10x10	-40 (dB) / -30 / -25 / -3 RSM-04	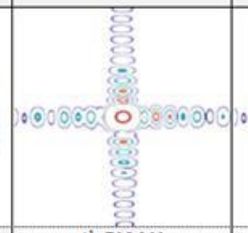	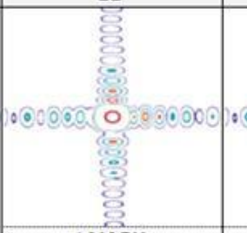	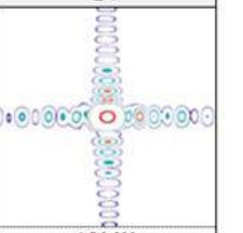
Total Processing Time		4h 7'30''	13'37''	12'6''
Speed-up Factor		-	18.18	20.46

(c)

Target	Height [m]	Range Resolution	Azimuth Resolution	Range PSLR	Azimuth PSLR	Range Shape 6dB/3dB	Range Shape 10dB/3dB	Azimuth Shape 6dB/3dB	Azimuth Shape 10dB/3dB	Ground Range Geolocation Error [m]	Azimuth Geolocation Error [m]	Angle of Incidence [deg]	Angle of Squint [deg]
RSM-03	660.9	0.957	0.804	-22.28	-23.88	1.380	1.720	1.381	1.723	-0.724	0.448	43.08	0.37
RSM-04	661.2	0.959	0.806	-23.37	-23.43	1.381	1.720	1.381	1.723	-0.654	0.463	43.11	0.36
RSM-05	661.2	0.958	0.807	-24.28	-23.10	1.380	1.720	1.381	1.723	-0.662	0.457	43.14	0.35
RSM-06	661.2	0.954	0.810	-23.59	-24.49	1.381	1.721	1.381	1.723	-0.650	0.429	43.17	0.33
RSM-07	661.3	0.958	0.808	-23.43	-24.36	1.381	1.721	1.381	1.723	-0.620	0.424	43.20	0.32

(d)

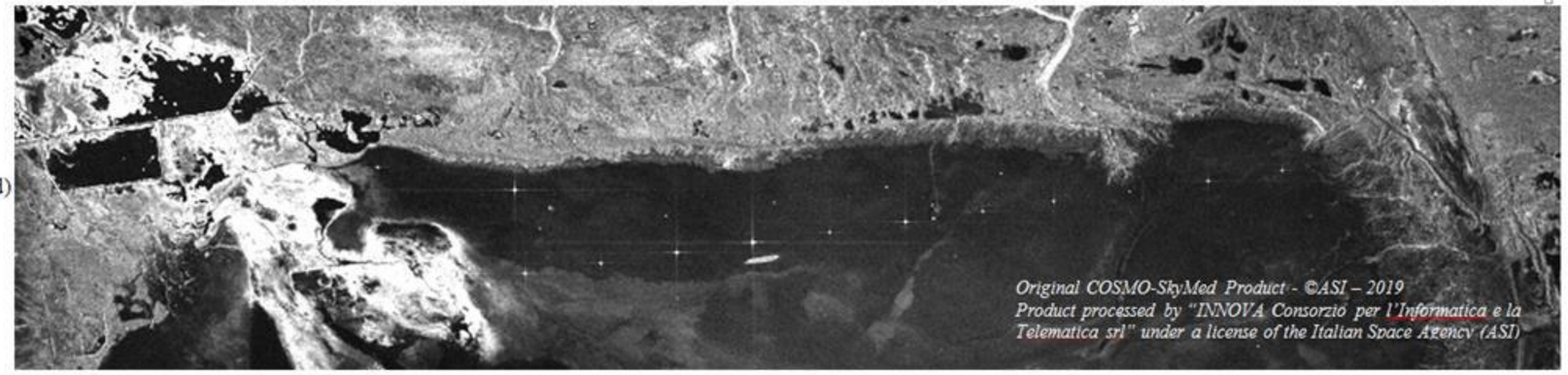

The proposed algorithm allows to reduce the total processing time for this data from more than 4 hours of standard processing to nearly 12 minutes when the optimizations are enabled.

Conclusions:

- The use of an algorithm in the time domain allows to achieve excellent focusing results even in the case of acquisitions with very challenging characteristics
- This focusing technique is independent from the radar wavelength and the size of the scenes, and it is particularly suitable for future SAR missions
- The algorithmic optimizations proposed and tested through software prototypes prove to be efficient and effective substantially reducing the computational burden and maintaining at the same time almost unchanged the quality of the image obtained compared to the not optimized standard TDBP processing
- The robustness of the implementation of the algorithm is under testing on a real image demonstrating its accuracy even in not ideal conditions
- The computational architecture of the software prototype has been design to achieve a very high degree of parallelization taking advantage of the recent HW multiprocessor/multicore architectures.
- The proposed TDBP algorithm, in both standard and optimized formulations, allows to focus small selected areas of the output image in proportionally reduced time allowing a local improvements in image quality with reduced hardware platform requirements that would make it suitable for use on a data analysis workstation.
- The independent focalization of each pixel allows to get the output image focused in the desired projection (e.g. Ground-Projected or Geocoded UTM/UPS) reducing the total execution time of the complete processing chain.
- The Proposed FAST-TDBP implementation it is also suitable to be used for airborne and sub orbital flights SAR acquisitions.

We thank the **Italian Space Agency (ASI)** for the opportunity to use COSMO-Skymed mission data for the development, testing and verification activities described above.

Thanks to the **Telespazio SPA** for its valuable contribution in terms of high quality simulated dataset used for the verification and testing activities of the proposed solution.

Thank You !

Z.I. La Martella, III Traversa G. B. Pirelli s.n. - 75100 Matera – Italy
Ph: +39 0835 307760 | +39 0835 1855118
www-consorzio-innova.com
tataranni@consorzio-innova.it

VH-RODA: Very High-resolution Radar & Optical Data Assessment workshop and CEOS SAR 2019 workshop